Omsite, $(Ni,Cu)_2Fe^{3+}(OH)_6[Sb(OH)_6]$, a new member of the cualstibite group from Oms, France

S. J. Mills[1,*], A. R. Kampf[2], R. M. Housley[3], G. Favreau[4], M. Pasero[5], C. Biagioni[5], S. Merlino[5], C. Berbain[6] and P. Orlandi[5]

[1] Geosciences, Museum Victoria, GPO Box 666, Melbourne, Victoria 3001, Australia
[2] Mineral Sciences Department, Natural History Museum of Los Angeles County, 900 Exposition Boulevard, Los Angeles, California 90007, USA
[3] Division of Geological and Planetary Sciences, California Institute of Technology, Pasadena, California 91125, USA
[4] 421 Avenue Jean Monnet, 13090 Aix-en-Provence, France
[5] Dipartimento di Scienze della Terra, Università di Pisa, Via S. Maria 53, I-56126 Pisa, Italy
[6] 32 rue R. Cassin, 66270 Le Soler, Pyrénées-Orientales, France

[*Received 5 July 2012; Accepted 13 August 2012; Associate Editor: G. Diego Gatta*]

ABSTRACT

Omsite (IMA 2012-025) is a new mineral from the Correc d'en Llinassos, Oms, Pyrénées-Orientales Department, France. It occurs as bright yellow to amber yellow discoidal tablets, flattened on {001}, which form rosettes typically 50–100 μm in diameter. Omsite generally crystallizes on siderite without associated supergene minerals; it occurs less commonly with glaukosphaerite. Crystals have a vitreous to resinous lustre, and are transparent to translucent. Omsite is not fluorescent in either short-wave or long-wave ultraviolet light. It has an estimated hardness of 3 on the Mohs' scale, is brittle with an irregular fracture, and has one poor cleavage on {001}. The calculated density is 3.378 g cm^{-3}. Crystals are uniaxial (–), with indices of refraction of $\omega = 1.728(3)$ and $\varepsilon = 1.66(1)$, measured in white light. Pleochroism is ω = orange-yellow, ε = pale orange-yellow; $\omega > \varepsilon$. The empirical formula [based on 12 (OH + Cl) p.f.u.] is $(Ni^{2+}_{1.099}Cu^{2+}_{0.665}Mg_{0.107}Fe^{3+}_{0.045})_{\Sigma 1.916}Fe^{3+}_{1.000}(Sb^{5+}_{0.947}As_{0.072}Na_{0.029})_{\Sigma 1.048}OH_{11.967}Cl_{0.033}$. Omsite crystallizes in space group $P\bar{3}$, with unit-cell parameters $a = 5.3506(8)$, $c = 19.5802(15)$ Å, $V = 485.46(10)$ Å^3 and $Z = 2$ determined by single crystal X-ray diffraction. The five strongest lines in the X-ray powder diffraction pattern [d in Å, (I_{rel}), (hkl)] are as follows: 4.901, (100), (004); 4.575, (83), (011); 2.3539, (81), (11$\bar{4}$); 1.8079, (48), (11$\bar{8}$); 3.781, (34), (103). The crystal structure was solved to $R_1 = 0.0896$ for 356 observed reflections [$F_o > 4\sigma F_o$] and 0.1018 for all the 469 unique reflections. Omsite is a layered double hydroxide (LDH) mineral, with a topology consistent with members of the hydrotalcite supergroup and cualstibite group.

Keywords: omsite, zincalstibite, cualstibite, hydrotalcite, layered double hydroxide, LDH, polytype, crystal structure.

Introduction

The first reference to mining activities at Oms in the Pyrénées-Orientales, France, dates from 1850 and mentions an iron deposit in the Correc d'en Llinassos or 'Llinassos Brook' (Berbain *et al*., 2005). Prospecting in the area between 1897 and 1907, was encouraged by the discovery of galena and stibnite in a nearby field. Between 1937 and 1939, operations were concentrated on the lower levels of Correc d'en Llinassos, where 50 m of galleries, two pits and 25 m of trench were excavated. Seventy tons of copper ore and a few

* E-mail: smills@museum.vic.gov.au
DOI: 10.1180/minmag.2012.076.5.16

tons of Ag-bearing galena were recovered. Catastrophic floods in 1940 destroyed the mine and backfilled the workings, which were abandoned. In 1941, the Compagnie des Mines de Moissac opened three trial adits on the siderite veins, but no ore was produced. In 1957, the BRGM (French Geological Survey) carried out surveys to assess the mining potential of the area (Autran and Azais, 1958). At Oms and other neighbouring mineralized areas, the projected ore reserves were considered insufficient to be of commercial interest, and subsequent activity was limited.

In 2005, during a systematic description of mineral localities in the Pyrénées-Orientales Department (Berbain *et al*., 2005), two of the authors (GF and CB) noticed that despite references to abundant ullmannite at the Correc d'en Llinassos, no Ni-bearing secondary minerals other than annabergite had been reported. A field trip to look for other Ni-bearing secondary minerals resulted in the discovery of the first French bottinoite, glaukosphaerite and the first specimens of a new Ni-, Cu-, Fe-, and Sb-bearing hydroxide (Berbain and Favreau, 2007). This new mineral is named omsite, for Oms, the closest village to the Correc d'en Llinassos locality. The mineral and name (IMA 2012-025) have been approved by the IMA Commission on New Minerals, Nomenclature and Classification (CNMNC). Two cotype specimens have been deposited in the collections of the Natural History Museum of Los Angeles County, Los Angeles, California, USA, under catalogue numbers 63428 and 63429, and one in the collections of Museum Victoria, Melbourne, Victoria, Australia, registration number M51584.

Occurrence and paragenesis

Omsite was found at the Correc d'en Llinassos, which is near the village of Oms in the Pyrénées-Orientales Department, France, 15 km north of the Spanish border (42º32′16″N 02º42′26″E). The village is located in the Aspres geological massif (in Catalan, 'aspres' describes arid soils that are hard to cultivate), which covers approximately 300 km^2, and consists mostly of shale, with minor limestone and sandstone (Beaumont and Guitard, 1954; Autran and Azais, 1958; Pigetvieux, 1981). Most of the metallic mineral occurrences (except for some karst iron localities) are located in Lower Ordovician Jujols Series rocks, which are largely shale and sandstone overlying a granitic basement. They are typically either sulfide impregnations or fault fillings associated with regional tectonic activity (Beaumont and Guitard, 1954; Autran and Azais, 1958; Pigetvieux, 1981). Numerous hydrothermal quartz veins crop out across the massif, but most contain no base metal mineralization, or only minor 'limonite'/goethite (Berbain and Favreau, 2007). Since the 1950s, Au, Sb and Zn anomalies have been identified (Beaumont and Guitard, 1954; Autran and Azais, 1958; Pigetvieux, 1981), but as yet no mining has occurred at any of these localities.

Omsite occurs in narrow, crystal-lined fractures in massive siderite-bearing rock (Fig. 1) with ullmannite and chalcopyrite, and less commonly with tetrahedrite/tennantite. Siderite occurs as flattened rhombohedra with stepped faces. Omsite generally crystallizes on siderite without associated supergene minerals; it occurs less commonly with glaukosphaerite, which forms pale green velvety balls up to 0.5 mm across (Fig. 2).

The secondary mineral assemblage is interpreted as having resulted from the decomposition of the primary sulfide minerals ullmannite, tetrahedrite/tennantite, sphalerite and chalcopyrite in mildly acidic conditions.

Physical and optical properties

Omsite most commonly occurs as curved discoidal tablets, which are flattened on {001}, and bounded by indistinct forms in the [001] zone, possibly including {100} and {110}. The tablets are commonly intergrown to form rosettes (Fig. 3), which are typically 50–100 μm across; the individual crystallites are generally no more

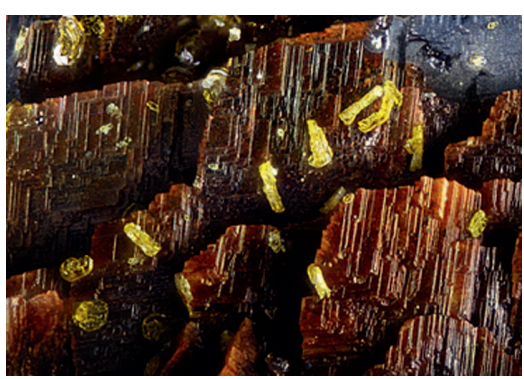

FIG. 1. Yellow tablets of omsite on siderite. The field of view is approximately 1 mm across.

FIG. 2. Yellow tablets of omsite with green balls of glaukosphaerite. The field of view is approximately 2 mm across.

than 10 μm thick. The same crystal habit was recently reported for crystals of zincalstibite-9*R* from Monte Avanza, Italy by Mills *et al.* (2012*b*). The colour of omsite ranges from bright yellow to amber yellow. The streak is pale yellow, the lustre is vitreous to resinous and crystals are transparent to translucent. Omsite is not fluorescent in either short-wave or long-wave ultraviolet light. It has a hardness estimated at 3 on the Mohs' scale (by analogy with cualstibite), is brittle with an irregular fracture, and has one poor cleavage on {001}. The density could not be measured because of the small size of the crystals and their near-invisibility in Clerici solution; the

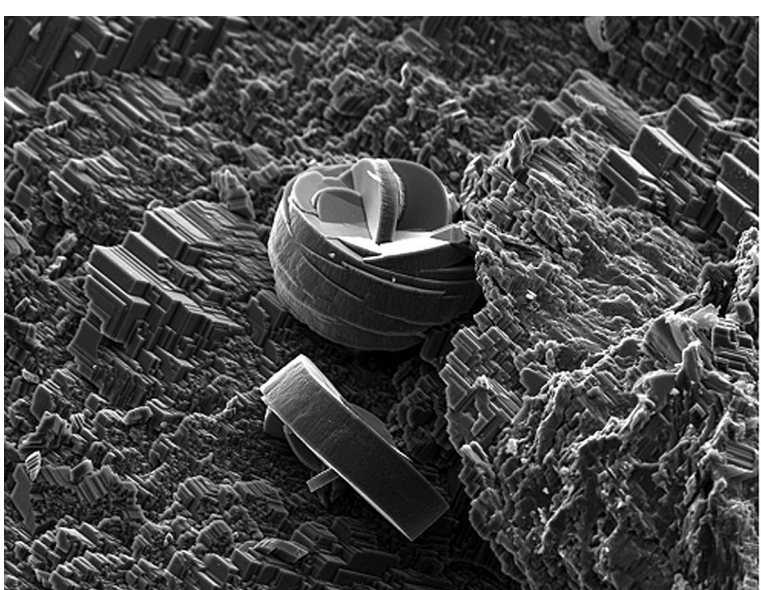

FIG. 3. Curved intergrown crystals of omsite forming rosettes on siderite. The field of view is approximately 100 μm across.

TABLE 1. Quantitative analytical data (mean of five analyses) for omsite.

Constituent	Mean (wt.%)	Range	SD	Probe standard
Na_2O	0.18	0.04–0.41	0.16	albite
MgO	0.86	0.63–1.28	0.30	forsterite
CuO	10.55	8.19–11.88	1.67	cuprite
NiO	16.37	15.34–18.35	1.33	synthetic NiO
Fe_2O_3	16.64	16.01–16.96	0.43	fayalite
Sb_2O_5	30.54	30.35–30.90	0.25	Sb metal
As_2O_5	1.66	1.20–1.93	0.32	GaAs
Cl	0.23	0.05–0.55	0.23	sodalite
O=Cl	−0.05			
H_2O_{calc}	21.50			
Total	98.48			

calculated density based on the empirical formula and single-crystal unit cell is 3.378 g cm^{-3}.

Optically, omsite is uniaxial (−), with indices of refraction of ω = 1.728(3) and ε = 1.66(1), measured in white light. Note that because of the small size and unfavourable orientation of the plates, ε could only be estimated based upon retardation measurements using a Berek compensator. Pleochroism is ω = orange-yellow, ε = pale orange-yellow; ω > ε.

Chemical composition

Quantitative chemical analyses (5) of omsite were carried out using a JEOL 8200 electron microprobe operating at 15 kV, 5 nA with a 5 μm beam diameter in wavelength-dispersive spectrometry (WDS) mode (Division of Geological and Planetary Sciences, California Institute of Technology). The analytical data were processed with the *CITZAF* correction procedure. Water could not be measured directly due to the paucity of material available, but was confirmed by the crystal-structure analysis. No other elements except those reported below were observed. The H_2O content was calculated on the basis of 12 (OH + Cl) p.f.u.; Na is placed in the interlayer with Sb and As, as in members of the wermlandite group (Mills *et al*., 2012*a*). Analytical data and standards are given in Table 1.

The empirical formula [based on 12 (OH + Cl) p.f.u.] is $(Ni^{2+}_{1.099}Cu^{2+}_{0.665}Mg_{0.107}Fe^{3+}_{0.045})_{1.916}Fe^{3+}_{1.000}(Sb^{5+}_{0.947}As_{0.072}Na_{0.029})_{1.047}OH_{11.967}Cl_{0.033}$. The ideal endmember formula is $Ni_2Fe^{3+}(OH)_6[Sb(OH)_6]$, which requires NiO 29.93, Fe_2O_3 16.00, Sb_2O_5 32.42, H_2O 21.65; total 100 wt.%.

Powder diffraction

The X-ray powder diffraction data for omsite were obtained on a Rigaku R-Axis Rapid II curved imaging plate microdiffractometer using

TABLE 2. X-ray powder diffraction data for omsite.

I_{meas}	d_{meas}	d_{calc}	I_{calc}	*h k l*
30	9.84	9.7901	19	0 0 2
100	**4.901**	4.8951	100	0 0 4
83	**4.575**	4.5092	29	0 1 1
34	**3.781**	3.7784	19	1 0 3
4	3.270	3.2634	2	0 0 6
9	3.008	2.9910	7	1 0 5
26	2.6853	2.6753	35	1 1 0
14	2.5768	2.5807	4	1 1 $\bar{2}$
21	2.5186	2.5175	4	0 0 8
81	**2.3539**	2.3476	66	1 1 $\bar{4}$
10	2.1634	2.1834	2	0 2 3
7	2.0732	2.0689	4	1 1 $\bar{6}$
20	1.9804	1.9940	3	2 0 5
		1.9693	2	1 0 9
48	**1.8079**	1.8058	35	1 1 $\bar{8}$
19	1.7484	1.7444	3	2 1 $\bar{1}$
5	1.6907	1.6916	3	2 1 3
8	1.6543	1.6616	1	1.0.11
3	1.5804	1.5800	1	1.1.10
16	1.5484	1.5446	10	3 0 0
11	1.5292	1.5257	2	3 0 2
24	1.4757	1.4730	13	0 3 4
18	1.3940	1.3930	10	1.1.12
8	1.3408	1.3377	4	2 2 0
15	1.3085	1.3062	5	0 3 8
13	1.2922	1.2903	6	2 2 4

The five strongest lines are listed in bold.

TABLE 3. Crystal data and details of data collection and structure refinement for omsite.

Crystal data	
Cell setting, space group	Trigonal, $P\bar{3}$
a (Å)	5.3506(8)
c (Å)	19.5802(15)
V (Å^3)	485.46(10)
Z	2
Data collection and refinement	
Radiation type, (λ)	Mo$K\alpha$ (0.71075 Å)
Temperature (K)	293
Maximum observed 2θ (º)	46.42
Measured reflections	6697
Unique reflections	469
Reflections $F_o>4\sigma F_o$	356
R_{int}	0.0885
R_σ	0.0373
Range of h, k, l	$-5 \leqslant h \leqslant 5$ $-5 \leqslant k \leqslant 5$ $-21 \leqslant l \leqslant 21$
R_1 [$F_o>4\sigma F_o$]	0.0896
R_1 (all data)	0.1018
wR_2 (on F_o^2)	0.2810
GooF	1.190
Number of l.s. parameters	69
Extinction coefficient	0.003(4)
$\Delta\rho_{max}$ and $\Delta\rho_{min}$	2.20, −1.722

The SXRD refinement parameters are as follows:
$R_{int} = \Sigma|F_o^2-F_o^2(\text{mean})|/\Sigma[F_o^2]$;
GooF = $S = \{\Sigma[w(F_o^2-F_c^2)^2]/(n-p)\}^{½}$;
$R_1 = \Sigma||F_o|-|F_c||/\Sigma|F_o|$;
$wR_2 = \{\Sigma[w(F_o^2-F_c^2)^2]/\Sigma[w(F_o^2)^2]\}^{½}$;
$w = 1/[\sigma^2(F_o^2) + (aP)^2 + bP]$ where a is 0.1929, b is 0 and P is $[2F_c^2 + \text{Max}(F_o^2,0)]/3$.

monochromatic Mo$K\alpha$ radiation. The observed powder d-spacings and relative intensities were derived by profile fitting using *JADE 9.1* software and these data are listed in Table 2. The space group and unit-cell parameters refined from the powder data using *JADE 9.1* with whole pattern fitting are: $P\bar{3}$, with a = 5.360(2), c = 19.589(7) Å, V = 487.3(1) Å^3 and Z = 2. The observed powder data are in excellent agreement with those calculated from the structure (Table 2).

Crystal structure

Single-crystal data were collected on the instrument described in the preceding section (Table 3). The Rigaku *CrystalClear* software package was used to process the diffraction data, including the

TABLE 4. Atom coordinates and displacement parameters (Å^2) for omsite.

Site	x/a	y/a	z/c	s.o.f.	U_{eq}	U_{11}	U_{22}	U_{33}	U_{23}	U_{13}	U_{12}
Sb1	0	0	0	⅙	0.040(1)	0.041(1)	0.041(1)	0.038(2)	0	0	0.021(1)
Sb2	⅔	⅓	0.4999(2)	0.141	0.036(1)	0.040(2)	0.040(2)	0.027(2)	0	0	0.020(1)
As2	⅔	⅓	0.4999(2)	0.025	0.036(1)	0.040(2)	0.040(2)	0.027(2)	0	0	0.020(1)
M1	0	0	0.2519(2)	0.301(7)	0.023(2)	0.022(2)	0.022(2)	0.025(2)	0	0	0.011(1)
M2	⅔	⅓	0.2488(2)	0.285(8)	0.021(2)	0.020(2)	0.024(2)	0.024(2)	0	0	0.010(1)
M3	⅓	⅔	0.2488(2)	0.289(8)	0.023(2)	0.021(2)	0.021(2)	0.025(2)	0	0	0.011(1)
O1	−0.331(2)	0.000(2)	0.1960(6)	1	0.020(3)	0.005(4)	0.008(4)	0.048(8)	0.001(3)	0.001(3)	0.004(3)
O2	0.340(2)	0.002(2)	0.3011(5)	1	0.038(4)	0.049(7)	0.049(7)	0.015(7)	0.001(4)	−0.001(4)	0.024(5)
O3a	0.475(5)	0.002(4)	0.443(1)	0.52(2)	0.040(5)	0.040(9)	0.050(11)	0.035(9)	−0.006(6)	0.001(6)	0.026(8)
O3b	0.193(10)	−0.136(11)	0.443(2)	0.25(2)	0.040(5)	0.040(9)	0.050(11)	0.035(9)	−0.006(6)	0.001(6)	0.026(8)
O3b′	0.325(10)	0.138(11)	0.443(2)	0.23(2)	0.040(5)	0.040(9)	0.050(11)	0.035(9)	−0.006(6)	0.001(6)	0.026(8)
O4a	0.141(5)	−0.199(5)	0.060(1)	0.52(2)	0.038(4)	0.044(8)	0.044(9)	0.027(7)	−0.003(6)	−0.004(6)	0.023(7)
O4b	−0.140(5)	−0.340(5)	0.060(1)	0.48(2)	0.038(4)	0.044(8)	0.044(9)	0.027(7)	−0.003(6)	−0.004(6)	0.023(7)

application of an empirical absorption correction. Streaking along the *c* axis contributed to a relatively high R_{int} of 0.0885, however, all of the non-H atoms were located. The heavy atoms were found using *SHELXS-97* (Sheldrick, 2008). The O atoms were then located via difference-Fourier syntheses. During the refinement it became apparent that the oxygen atom sites in the $[Sb(OH)_6]$ layers, O3 and O4, were split. The temperature factors of the split sites were constrained to be the same, whereas their occupancies were freely refined. The O3 site was split into three sub-sites, O3a, O3b, and O3b′, with refined occupancies of 0.52(2):0.25(2):0.23(2). The O4 site was split into two sub-sites, O4a and O4b, with occupancies of 0.52(2):0.48(2). The Sb1–O bond-lengths are reasonable for Sb^{5+} in octahedral coordination (Mills *et al*., 2009), whereas those for the Sb2 octahedron are relatively short. This is consistent with some substitution of As^{5+} for Sb at the Sb2 site. We could not locate a separate site in the interlayer for the Na atom, which forms a $[Na(H_2O)_6]$ octahedron in wermlandite-group minerals (Rius and Allmann, 1984; Mills *et al*., 2012*a*). Owing to the similar scattering factors of Ni, Cu, and Fe, the site occupancies of the three independent metal sites in the brucite-like layer were freely refined using the scattering factor of Ni. The refined site occupancies are a little lower than the ideal full occupancy, which is consistent with minor substitution by lighter atoms, particularly Mg.

The final model, anisotropically refined, converged to R_1 = 0.0896 for 356 observed reflections [$F_o > 4\sigma F_o$] and 0.1020 for all 469 unique reflections. In the final difference-Fourier map, the two highest maxima (2.2 and 1.9 *e* Å^{-3}) are located at (0,0,½) and (⅔,⅓,0), corresponding to the empty octahedral positions in the $[Sb2(OH)_6]$ and $[Sb1(OH)_6]$ layers, respectively. Details of the data collection and structure refinement are shown in Table 3. Final atom coordinates, site occupancies and displacement parameters are reported in Table 4. Selected bond distances are provided in Table 5. A crystallographic information file has been deposited with the Principal Editor of *Mineralogical Magazine* and is available at http://www.minersoc.org/pages/e_journals/dep_mat.html.

Description of the structure

Omsite can be considered to be a layered double hydroxide (LDH) mineral, with a topology that is consistent with members of the hydrotalcite supergroup and cualstibite group (Mills *et al*., 2012*a*). Unit-cell parameters are consistent with a 2*T* polytype with a $\sqrt{3} \times \sqrt{3}$ superstructure in the *xy* plane. The structure of omsite consists of a $(Ni,Cu)_2Fe(OH)_6$ brucite-like layer, with $Sb(OH)_6$ octahedra in the interlayer. The $Sb(OH)_6$ octahedra are split into two statistically occupied positions, related by a 60º rotation (Fig. 4). It is interesting to note that both cualstibite and zincalstibite have partially occupied $Sb(OH)_6$ octahedra within the interlayer (Bonaccorsi *et al*., 2007; Mills *et al*., 2012*b*). As with zincalstibite-9*R* (Mills *et al*., 2012*b*), omsite shows very little evidence of cation ordering in the *M* sites. All of the metal sites have a similar mean bond distance of 2.05±0.02 Å (Table 5), and the coordination octahedra are relatively regular, with bond-distance variations of only

TABLE 5. Selected bond distances (Å) in omsite.

Sb1–O4a	1.971(19) ×6	*M*1–O2	2.053(10) ×3
Sb1–O4b	1.974(21) ×6	*M*1–O1	2.081(9) ×3
<Sb1–O>	**1.973**	**<*M*1–O>**	**2.067**
Sb2–O3a	1.904(20) ×3	*M*2–O2	2.039(10) ×3
Sb2–O3b′	1.908(42) ×3	M2–O1	2.068(8) ×3
Sb2–O3b	1.916(40) ×3	**<*M*2–O>**	**2.054**
Sb2–O3a	1.919(21) ×3		
<Sb2–Oa>	**1.912**	*M*3–O2	2.051(10) ×3
<Sb2–Ob*>	**1.912**	*M*3–O1	2.068(8) ×3
		<*M*3–O>	**2.060**

* Including both b and b′.

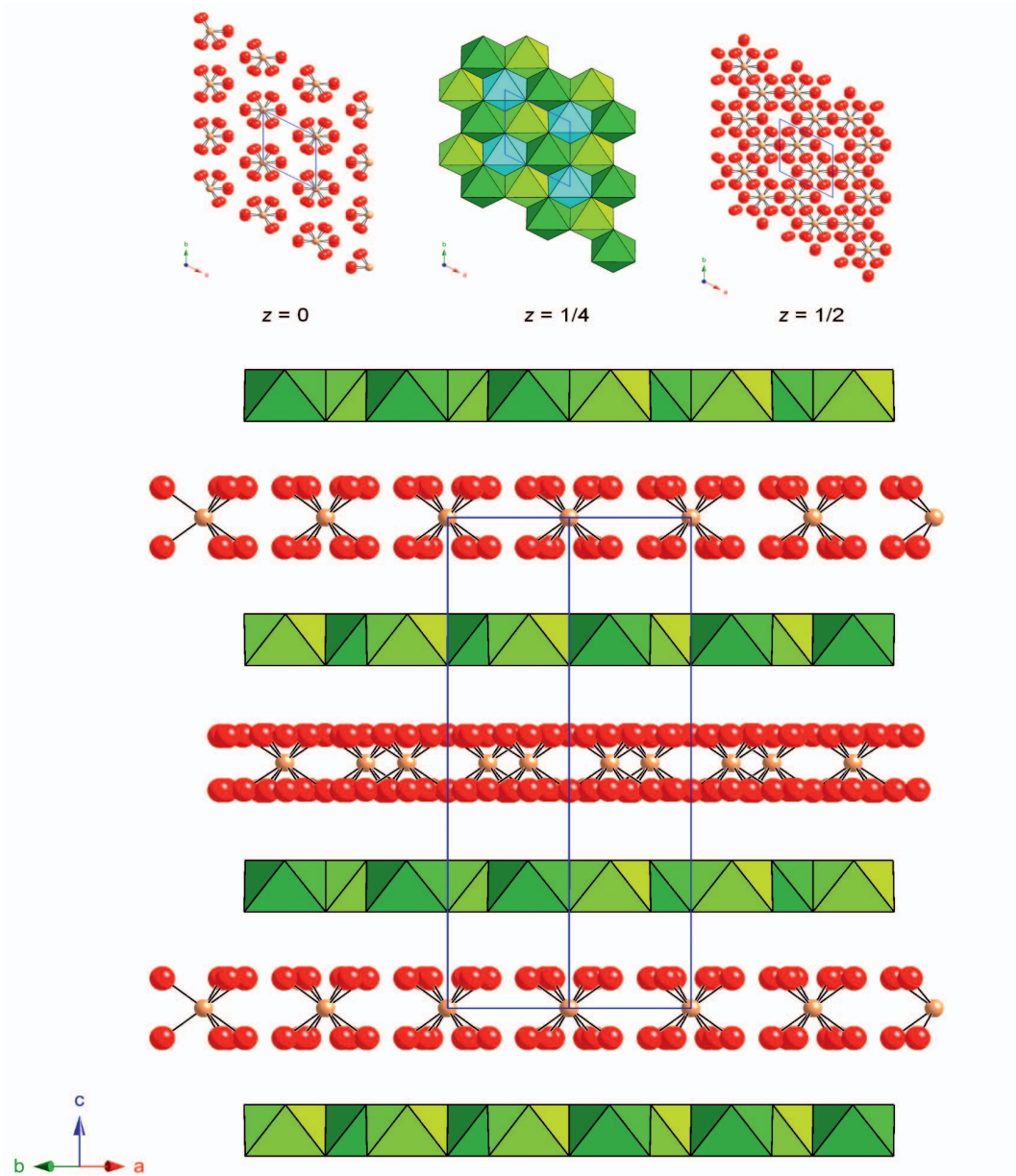

FIG. 4. The crystal structure of omsite: $M1O_6$ octahedra are light blue, $M2O_6$ octahedra are dark green and $M3O_6$ octahedra are light green; interlayer Sb atoms are orange and partially occupied OH groups are red. View of the layers at z = 0, ¼, and ½ (top) and down [110] (bottom). The unit cell is indicated with blue lines.

0.028, 0.029 and 0.017 Å for *M*1, *M*2 and *M*3, respectively, implying that there is no Jahn–Teller distorted environment into which Cu^{2+} might partition. It is nevertheless possible that cation ordering occurs within individual layers, but that there is poor correlation between layers, as is the case for some other members of the hydrotalcite supergroup (Mills *et al*., 2012*a*).

The diversity in polytypes within the cualstibite group is interesting. As noted above, omsite

occurs as the 2*T* polytype with a $\sqrt{3} \times \sqrt{3}$ superstructure, whereas zincalstibite has been reported as the 1*T* polytype with a $\sqrt{3} \times \sqrt{3}$ superstructure by Bonaccorsi *et al*. (2007) and as the 9*R* polytype with the same superstructure by Mills *et al.* (2012*b*). Cualstibite has been reported with a 1*T* polytype, but with a 3×3 superstructure (Walenta, 1984; Bonaccorsi *et al*., 2007), whereas Kolitsch and Giester (2007) and Kolitsch *et al*. (in press) reported the 1*M* polytype (= cyanophyllite, see Mills *et al*., 2012*a* for further details). It is not clear why the cualstibite group has more structural diversity than other groups within the hydrotalcite supergroup; the well formed crystals and $Sb(OH)_6$ octahedral interlayer may play a significant role. The lack of suitable crystals for single-crystal determination remains a hurdle in the characterization of many of the minerals in the hydrotalcite supergroup.

Acknowledgements

Referees Gunnar Raade, Uwe Kolitsch and Andy Christy are thanked for their helpful comments on the manuscript. Part of this study was funded by the John Jago Trelawney Endowment to the Mineral Sciences Department of the Natural History Museum of Los Angeles County. The microprobe analyses were supported by a grant to the California Institute of Technology from the Northern California Mineralogical Association. Jean-Marc Johannet is thanked for the colour photography.

References

Autran, A. and Azais, H. (1958) *Résultats des travaux effectués dans les Aspres*. BRGM Report A1376. BRGM, Orléans, France.

Beaumont, C. and Guitard, G. (1954) *Introduction à l'étude du district cuprifère des Aspres*. BRGM Report A740. BRGM, Orléans, France.

Berbain, C. and Favreau, G. (2007) Un exemple peu courant de minéralisation nickélifère: le Correc d'en Llinassos à Oms (Pyrénées-Orientales). *Le Cahier des Micromonteurs*, **95**, 3–24.

Berbain, C., Favreau, G. and Aymar, J. (2005) *Mines et Minéraux des Pyrénées-Orientales et des Corbières*. Association Française de Microminéralogie, France, 250 pp.

Bonaccorsi, E., Merlino, S. and Orlandi, P. (2007) Zincalstibite, a new mineral, and cualstibite: crystal chemical and structural relationships. *American Mineralogist*, **92**, 198–203.

Kolitsch, U. and Giester, G. (2007) A preliminary determination of the crystal structure of cyanophyllite and revision of its chemical formula. *Mitteilungen der Österreichischen Mineralogischen Gesellschaft*, **153**, 66, [from abstract].

Kolitsch, U., Giester, G. and Pippinger, T. (in press) The crystal structure of cualstibite-1M (formerly cyanophyllite), its revised chemical formula and its relation to cualstibite-1T. *Mineralogy and Petrology*.

Mills, S.J., Christy, A.G., Chen, E.C.-C. and Raudsepp, M. (2009) Revised values of the bond valence parameters for $^{[6]}Sb(V)–O$ and $^{[3-11]}Sb(III)–O$. *Zeitschrift für Kristallographie*, **224**, 423–431.

Mills, S.J., Christy, A.G., Génin, J.-M.R., Kameda, T. and Colombo, F. (2012*a*) Nomenclature of the hydrotalcite supergroup: natural layered double hydroxides. *Mineralogical Magazine*, **76**, 1289–1336.

Mills, S.J., Christy, A.G., Kampf, A.R., Housley, R.M., Favreau, G., Boulliard, J.-C. and Bourgoin, V. (2012*b*) Zincalstibite-9*R*: the first nine-layer polytype with the layered double hydroxide structure-type. *Mineralogical Magazine*, **76**, 1337–1345.

Pigetvieux, G. (1981) *Etude Géologique et Métallogénique des Aspres*. Unpublished PhD thesis. Université de Franche-Comté, Besançon, France.

Rius, J. and Allmann, R. (1984) The superstructure of the double layer mineral wermlandite $[Mg_7(Al_{0.57}Fe^{3+}_{0.43})_2(OH)_{18}]^{2+}[(Ca_{0.6}Mg_{0.4})(SO_4)_2(H_2O)_{12}]^{2-}$. *Zeitschrift für Kristallographie*, **168**, 133–144.

Sheldrick, G.M. (2008) A short history of *SHELX*. *Acta Crystallographica*, **A64**, 112–122.

Walenta, K. (1984) Cualstibit, ein neues Sekundärmineral aus der Grube Clara im mittleren Schwarzwald (BRD). *Chemie der Erde*, **43**, 255–260.